HHS Public Access

Author manuscript

Oncogene. Author manuscript; available in PMC 2017 September 20.

Published in final edited form as:

Oncogene. 2017 July 20; 36(29): 4150–4160. doi:10.1038/onc.2017.44.

The histone demethylase KDM3A, and its downstream target MCAM, promote Ewing Sarcoma cell migration and metastasis

Marybeth Sechler[1,4], **Janet K. Parrish**[2,4], **Diane K. Birks**[3,4], and **Paul Jedlicka**[1,2,4,*]

[1]Cancer Biology Graduate Training Program

[2]Department of Pathology

[3]Department of Neurosurgery

[4]University of Colorado Denver, Anschutz Medical Campus, Aurora CO

Abstract

Ewing Sarcoma is the second most common solid pediatric malignant neoplasm of bone and soft tissue. Driven by EWS/Ets, or rarely variant, oncogenic fusions, Ewing Sarcoma is a biologically and clinically aggressive disease with a high propensity for metastasis. However, the mechanisms underpinning Ewing Sarcoma metastasis are currently not well understood. In the present study, we identify and characterize a novel metastasis-promotional pathway in Ewing Sarcoma, involving the histone demethylase KDM3A, previously identified by our laboratory as a new cancer-promoting gene in this disease. Using global gene expression profiling, we show that KDM3A positively regulates genes and pathways implicated in cell migration and metastasis, and demonstrate, using functional assays, that KDM3A promotes migration *in vitro* and experimental, post-intravasation, metastasis *in vivo*. We further identify the Melanoma Cell Adhesion Molecule (MCAM) as a novel KDM3A target gene in Ewing Sarcoma, and an important effector of KDM3A pro-metastatic action. Specifically, we demonstrate that MCAM depletion, like KDM3A depletion, inhibits cell migration *in vitro* and experimental metastasis *in vivo*, and that MCAM partially rescues impaired migration due to KDM3A knock-down. Mechanistically, we show that KDM3A regulates MCAM expression both through a direct mechanism, involving modulation of H3K9 methylation at the MCAM promoter, and an indirect mechanism, via the Ets1 transcription factor. Lastly, we identify an association between high MCAM levels in patient tumors and poor survival, in two different Ewing Sarcoma clinical cohorts. Taken together, our studies uncover a new metastasis-promoting pathway in Ewing Sarcoma, with therapeutically targetable components.

*Corresponding author: Department of Pathology, University of Colorado Denver, Anschutz Medical Campus, 12800 E. 19th Ave., MS 8104, Aurora CO 80045. Phone: 303-724-8161. Fax: 303-724-3712. paul.jedlicka@ucdenver.edu.

Conflicts of Interest:

The authors have no conflicts of interest to disclose.

Supplementary Information accompanies the paper on the Oncogene website (http://www.nature.com/onc)

Keywords

Ewing sarcoma; migration; metastasis; epigenetics; Jumonji; histone; demethylase; KDM3A; MCAM; Ets

Introduction

Ewing Sarcoma is the second most common malignant bone and soft tissue tumor occurring in pediatric patients, with almost 200 new cases diagnosed in the United States every year [1]. It is a biologically aggressive, poorly differentiated neoplasm, with a high propensity for metastatic dissemination and relapse [2]. Although 70% of cases present with clinically localized tumors, all patients are treated as having micrometastatic disease at presentation, and therefore additionally receive multi-agent chemotherapy [2]. Approximately 30% of these initially clinically localized cases will relapse, frequently with metastatic disease [3]. These cases, along with the 30% of patients with metastatic disease upon diagnosis, have an average 5-year survival of less than 20% [4]. Currently, few targeted therapies are in clinical trials for the treatment of Ewing Sarcoma, and these have met with limited success [5, 6]. Given the tragic statistics of metastatic Ewing Sarcoma, new therapies that could combat tumor metastasis could be of particular benefit in this disease.

Ewing Sarcoma is a prototypical fusion oncogene-driven cancer. The vast majority of Ewing Sarcomas are characterized by an acquired chromosomal translocation involving a TET family member, most commonly the EWS gene on chromosome 22, and an Ets family transcription factor gene, the latter being Fli1 on chromosome 11 in 85% of cases [7]. EWS/Ets fusions yield a potent transcription factor, which is able to promote or suppress the expression of many genes depending on the promoter context [8–10]. EWS/Ets fusions are key drivers of Ewing Sarcoma pathogenesis, as fusion silencing results in growth arrest and apoptosis [11]. However, directly targeting the fusion in a clinical setting, though a long-standing goal in the field, remains to be effectively achieved to date. Moreover, the role that EWS/Ets fusions play in the biology of Ewing Sarcoma metastasis is at present unclear. Indeed, recently published studies suggest that EWS/Ets fusions may not be the chief drivers of metastatic phenotypes [12–14]. If this is the case, identification and understanding of other factors and pathways that promote Ewing Sarcoma metastasis assumes critical importance.

Epigenetic dysregulation has recently emerged as a very important mechanism of tumor initiation and progression [15], with an especially important role in pediatric cancers [16]. Recently, our laboratory identified the Jumonji-domain histone demethylase KDM3A, an epigenetic regulator, as a novel oncogene downstream of EWS/Fli1 in Ewing Sarcoma [17]. Namely, we showed that KDM3A is upregulated downstream of EWS/Fli1 in part through a microRNA-mediated mechanism, and that this upregulation promotes colony and tumor growth. In the present study, we define a new role for KMD3A in promoting Ewing Sarcoma cell migration and metastasis, identify the Melanoma Cell Adhesion Molecule (MCAM/CD146/MUC18) as a novel downstream target of KDM3A regulation and an important effector of its metastasis-promotional activity, and define mechanisms by which KDM3A augments MCAM expression. Together, these findings delineate a new metastasis-promoting

pathway in Ewing Sarcoma, with two pharmacologically targetable components, the histone demethylase KDM3A and the cell surface protein MCAM.

Results

KDM3A positively regulates metastasis-associated genes in Ewing Sarcoma

Our previous work identified KDM3A as a novel oncogene in Ewing Sarcoma [17]. To further investigate the molecular role of KDM3A in this disease, we performed microarray profiling of RNA isolated from A673 cells stably transduced with Scrambled shRNA control and two different shRNAs targeting KDM3A, using an Affymetrix whole transcript array (Human Gene 1.1 ST), in order to identify KDM3A-regulated genes. This analysis revealed 131 transcripts downregulated 1.5-fold or greater upon KDM3A knock-down with both shRNAs, compared to the Scrambled control (Supplemental Table 1). Interestingly, functional annotation analysis showed genes downregulated upon KDM3A knock-down to cluster into multiple biological process groups potentially relevant to cancer, including cell adhesion, cell motility/migration, vascular development and receptor signaling (Figure 1A and Supplemental Table 2). Expression profiling also revealed 60 upregulated transcripts (1.5-fold or greater) upon KDM3A knock-down (Supplemental Table 1), which showed significant clustering with one functional annotation group, developmental processes (Supplemental Table 2). The finding that KDM3A, a known activator of gene expression through removal of repressive H3K9 histone methyl 1 and 2 marks, positively regulates genes involved in cell adhesion suggested a possible basis for its colony growth-promoting role, shown in our previous studies [17]. Intriguingly, positive regulation of genes related to cell adhesion *and* cell motility/migration, processes frequently associated with tumor metastasis, further suggested to us a potential, previously unexplored, role of KDM3A in Ewing Sarcoma metastasis. Indeed, examination of the most significantly downregulated genes upon KDM3A knock-down (FDR (false discovery rate) < 0.1; Figure 1B), revealed, out of 13 total genes, 7 genes previously implicated in the promotion of metastasis in other cancers (CD44, MCAM, CTGF, CD9, RGNEF, SERPINE1 and KLF5[18–31]). Further, examination of changes in expression of specific genes contributing to the biological process groups in Figure 1A, revealed two-fold or greater downregulation, upon KDM3A knock-down, of 12 genes previously linked to metastasis in other cancers [18–49] (Figure 1C; of note, TNC has recently been shown to be metastasis-promotional in Ewing Sarcoma[14]). Taken together, our expression profiling studies suggested that KDM3A could represent a novel metastasis promoter in Ewing Sarcoma, via regulation of a pro-metastatic gene expression program.

KDM3A promotes Ewing Sarcoma cell migration, and experimental metastasis in vivo

To evaluate a potential functional role for KDM3A in Ewing Sarcoma metastasis, we next assessed whether manipulation of KDM3A levels alters metastatic phenotypes. We examined cell migration as a well-established, metastasis-associated process amenable to experimental analysis, and one affected by KDM3A in our expression profiling studies (Figure 1A). To assess migration, two Ewing Sarcoma cell lines (A673 and TC32) were each stably transduced with two different KDM3A-targeting shRNAs or Scrambled control shRNA, were plated in a Boyden chamber, and transwell migration was quantified at 12

hours. In both cell lines, cells with KDM3A knock-down (Figure 2, A and C) showed approximately a 50 percent decrease in migration compared to those harboring the Scrambled control (Figure 2, B and D). We further independently assessed cell migration using a wound-healing assay. This assay requires cells to grow in an adherent monolayer, an experimental condition optimally satisfied by A673 cells. As was the case with the Boyden chamber assay, A673 cells with KDM3A knock-down showed impaired migration into the wound compared to the Scrambled controls, again by an average of approximately 50 percent (Supplemental Figure 1). Together, these data support a migration-promoting role for KDM3A in Ewing Sarcoma.

We next examined whether KDM3A impacts metastasis in an experimental model *in vivo.* We selected the tail-vein injection model for these studies, as this model is well-established, readily quantifiable and relatively rapid (and thus less vulnerable to loss of effective knock-down of gene expression over time). Moreover, this model evaluates the later, post-intravasation, stages of metastasis (cell survival in the circulation, extravasation, tissue/organ seeding and metastasis outgrowth), which, from a potential therapeutic standpoint, are particularly relevant to Ewing Sarcoma, a disease presumed to have undergone at least microscopic spread beyond the primary site at clinical presentation. Animals injected with A673 cells harboring a KDM3A-targeting shRNA developed an approximately 10-fold lower metastatic tumor burden compared to animals injected with Scrambled shRNA control cells (Figure 3). These results support a role for KDM3A in the promotion of Ewing Sarcoma metastasis *in vivo*.

Taken together, our gene expression profiling analyses, along with our functional studies *in vitro* and *in vivo*, support a previously undefined role for KDM3A in Ewing Sarcoma metastasis.

MCAM is an effector of KDM3A pro-metastatic action in Ewing Sarcoma

In order to further understand the role of KDM3A in Ewing Sarcoma metastasis, we next examined which downstream genes could specifically be contributing to its metastasis-promotional effects. Returning to our microarray data (Figure 1), we noted the Melanoma Cell Adhesion Molecule (MCAM) to be one of the genes most strongly regulated by KDM3A. MCAM has been shown to promote metastasis in other types of cancer [50]. Moreover, in a meta-analysis of gene expression profiling data, MCAM was recently identified as one of the most commonly upregulated cell surface proteins (compared to normal tissue) in pediatric cancers, including Ewing Sarcoma [51]. Together, these findings suggested that MCAM could be a biologically, and potentially clinically, significant mediator of KDM3A metastasis-promotional effects in Ewing Sarcoma. In order to verify our expression profiling results and determine whether KDM3A is a more general regulator of MCAM expression in Ewing Sarcoma, we examined the effects of KDM3A knock-down on MCAM levels in multiple Ewing Sarcoma cell lines, including A673 and TC32 cells. These studies revealed consistent downregulation of MCAM levels upon KDM3A knock-down (Figure 4), indicating that KDM3A is an important regulator of MCAM expression in Ewing Sarcoma.

To further evaluate MCAM as a candidate downstream effector of KDM3A pro-metastatic action, we examined whether MCAM knock-down could phenocopy the effects of KDM3A depletion. We first examined cell migration using the same cell lines (A673 and TC32) and experimental approaches used above for KDM3A functional studies. In a Boyden chamber assay, upon MCAM knock-down using two different targeting shRNAs (Figure 5A and C), MCAM depletion resulted in diminished migration compared to cells with the Scrambled control, by approximately 50 percent in A673 cells and 30 percent in TC32 cells (Figure 5B and D). MCAM knock-down also resulted in diminished cell migration by an average of 60 percent in a wound-healing assay (Supplemental Figure 2). Lastly, forced re-expression of MCAM in the context of KDM3A depletion resulted in partial rescue of cell migration (Supplemental Figure 3), indicating that upregulation of MCAM is in part responsible for KDM3A pro-migratory effects.

We further assessed the effects of MCAM depletion on metastasis *in vivo*, using the tail vein experimental metastasis model. Mice injected with MCAM knock-down cells developed an approximately 3-fold lower metastatic tumor burden compared to those injected with the Scrambled control cells (Figure 6). Taken together, the above *in vitro* and *in vivo* studies indicate that MCAM, like KDM3A, is a promoter of metastasis in Ewing Sarcoma, and that MCAM contributes to KDM3A pro-metastatic effects.

MCAM expression is subject to both direct and indirect regulation by KDM3A, and high MCAM levels in patient tumors are associated with poor outcome

In order to understand how KDM3A regulates MCAM expression, we first examined whether this occurs through a direct mechanism. Using chromatin immunoprecipitation (ChIP) followed by qPCR, with KDM3A antibody and IgG negative control, we found that KDM3A specifically interacted with the genomic region flanking the MCAM transcription start site in Scrambled control cells, and that this interaction was diminished in KDM3A knock-down cells, consistent with KDM3A localization to the MCAM promoter (figure 7A). Further, using ChIP for the H3K9me2 mark negatively regulated by KDM3A, we found that levels of this mark in the same region increased upon KDM3A knock-down (Figure 7A). As an additional control, ChIP for KDM3A at a distal region (10 Kbp upstream of the MCAM transcription start site), revealed neither evidence of specific KDM3A localization, nor changes in levels of the H3K9me2 mark upon KDM3A knock-down (Figure 7B). Together, these data support a mechanism whereby KDM3A, at least in part, regulates MCAM expression directly, through interaction with the MCAM promoter region and H3K9 demethylation. We further queried whether the Ets1 transcription factor, which we found to be positively regulated by KDM3A in our expression analysis (Figure 1A), could also contribute to the control of MCAM levels. We had previously shown regulation of Ets1 expression by KDM3A in multiple Ewing Sarcoma cell lines, including A673 cells [17], and verified that this also holds true in TC32 cells (Supplemental Figure 4A). To examine a possible role for Ets1 in the control of MCAM expression, we stably depleted Ets1 levels in A673 cells, and assessed MCAM expression at both mRNA and protein levels. This analysis revealed potent downregulation of MCAM upon Ets1 knock-down (Figure 7C), demonstrating that Ets1 contributes to control of MCAM expression. Similarly, we found that Ets1 depletion in TC32 cells also resulted in diminished MCAM levels (Supplemental

Figure 4B). Moreover, in further support of this regulatory mechanism, we identified significant correlation between Ets1 and MCAM levels in patient tumors from two different publicly available Ewing Sarcoma clinical cohorts [52] (Figure 7D). Next, we asked whether KDM3A regulates Ets1 directly, and whether the same is true for regulation of MCAM by Ets1. Using ChIP-qPCR approaches analogous to those above, we found that KDM3A specifically interacts with the genomic region flanking the Ets1 transcription start site, and that KDM3A depletion results in augmented H3K9me2 levels in the same region (Figure 7E), consistent with direct regulation of Ets1 expression through H3K9 demethylation by KDM3A. Further, using ChIP-qPCR for Ets1, we found that Ets1 specifically interacted with an MCAM upstream regulatory region containing multiple candidate Ets binding sites, and that this interaction was abolished upon Ets1 knock-down (Figure 7F), thus supporting a direct mechanism for this regulatory relationship as well. Taken together, our data support a mechanism whereby KDM3A regulates MCAM expression both directly, as well as indirectly through control of Ets1 expression. Lastly, in support of the clinical relevance of our findings and an important role for MCAM in Ewing Sarcoma biology, interrogation of the same Ewing Sarcoma patient cohorts [52] revealed a significant association between high MCAM expression in tumors and poor survival (Figure 8). We were not able to demonstrate a significant correlation between KDM3A and MCAM expression, or a significant association between KDM3A expression and survival, in these same cohorts. This could be due to the relatively limited cohort size (46 and 39 total patients, respectively), but could also reflect more complex regulation of MCAM expression in tumors, including involvement of other EWS/Fli1-driven pathways (see Discussion). While further evaluation of relationships between KDM3A expression and disease outcomes is needed, the survival data from these cohorts underscore an important role for MCAM in high-risk disease.

Discussion

We have shown previously that the histone demethylase KDM3A is upregulated downstream of the EWS/Fli1 oncofusion, and promotes colony and tumor growth in Ewing Sarcoma [17]. In the present study, we show that KDM3A upregulates metastasis-promoting pathways and functionally augments Ewing Sarcoma cell migration *in vitro* and experimental, post-intravasation, metastasis *in vivo*, and identify the Melanoma Cell Adhesion Molecule (MCAM) as a novel KDM3A target and important mediator of these effects. Together, our prior and current studies support a role for KDM3A as an important promoter of malignant phenotypes in Ewing Sarcoma. Further, the current studies highlight an important, and clinically relevant, role for MCAM in the biology of Ewing Sarcoma.

Epigenetic modifiers have been increasingly implicated in cancer, including the malignant biology of Ewing Sarcoma [17, 53–57]. While our studies are the first to uncover a role for KDM3A in Ewing Sarcoma, this factor has recently also been noted as an important promoter of tumorigenesis and/or metastasis in other cancers [58–60, 61]. Interestingly, in neuroblastoma, another pediatric cancer, KDM3A was recently found to be upregulated by the oncogenic driver N-myc. KDM3A was shown to demethylate the promoter of the long non-coding RNA MALAT1, which resulted in an increase in MALAT1 levels, and in the metastasis-associated phenotypes of cell migration and invasion [62]. This study, while uncovering an entirely different molecular mechanism, bears interesting similarity to our

findings in Ewing Sarcoma, whereby the driver oncogene (in our case EWS/Fli1) upregulates KDM3A to promote tumor cell metastatic properties. Another interesting parallel emerges from recent studies in multiple myeloma, where KDM3A was shown to upregulate the KLF2 transcription factor, which in turn increased IRF4 expression, resulting in increased adhesion of cells to bone marrow stroma and protection from apoptosis [63]. It will be interesting to see whether induction of downstream transcription factors to effect and/or reinforce target regulation represents a more common mechanism of action of KDM3A in cancer.

In normal biology, MCAM is involved in many cellular processes, including cell adhesion [64], angiogenesis [65], cell survival [66], and extravasation [67]. These same processes are known to contribute to neoplasia and tumor progression, and MCAM expression has been shown to correlate with poor prognosis, metastasis and disease progression in a number of different cancer types, including melanoma, prostate, ovarian, gastric, non-small cell lung, gallbladder, and breast cancers [50, 68]. Mechanistically, expression of MCAM has been associated with phenotypes of epithelial-mesenchymal transition (EMT) [69, 70], increased cell extravasation [71] and increased metastasis in cell line models [50]. As mentioned earlier, a recent gene expression meta-analysis revealed MCAM to be one of the most prevalently overexpressed genes coding for factors expressed on the cell surface in common pediatric cancers, compared to normal tissue [51]. Thus, MCAM may play important roles in the malignant biology not just of Ewing Sarcoma, but other pediatric cancers.

Few studies to date have examined mechanisms of regulation of MCAM expression in cancer. In melanoma, recent studies have shown that MCAM is transcriptionally repressed by ZBTB7A [72], while in osteosarcoma, MCAM expression is in part controlled by the YY1 transcription factor [73]. Here we identify a new mechanism whereby MCAM is a regulatory target of the histone demethylase KMD3A both directly and indirectly via the action of Ets1. Ets1 is known to be overexpressed in many cancers [74]. Moreover, as an alternative mechanism for increased Ets1 regulatory action, promoter mutations generating gain-of-function Ets1 binding sites have recently been identified [75]. Lastly, growing evidence suggests that KDM3A itself is relatively frequently overexpressed in cancer [76–79]. Thus, the KDM3A/Ets1/MCAM axis, identified in our studies, may represent a more general mechanism of MCAM overexpression in cancer. Similarly, it will be interesting to determine whether Ets1 itself, a long-established tumor/metastasis promoter in adult cancers [40], plays important roles in pediatric neoplasia. In adult cancers, Ets1 has especially been linked to tumor progression including metastasis, via various mechanisms, including transcriptional upregulation of Matrix Metalloproteases (MMPs), the angiogenesis-promoting factor VEGF, and migration promoters such as Plasminogen Activator Inhibitor 1 (PAI-1) (reviewed in [40]). With respect to Ewing Sarcoma specifically, another intriguing possibility is that Ets1, a member of the EWS fusion partner transcription factor family with overlapping DNA-binding specificity, may directly impact DNA-binding and transcriptional regulation by EWS/Ets fusions.

Recent studies have raised many questions about the molecular driving forces behind Ewing Sarcoma metastasis. Notably, EWS/Ets fusions have been found to repress, rather than activate, many genes and biological processes known to be involved in the promotion of

metastatic phenotypes, such as cell adhesion and migration[12, 13]. This has led to a hypothesis that Ewing Sarcoma metastasis could in part be a passive process [12]. At the same time, however, others have described pathways that promote Ewing Sarcoma metastasis and antagonize the above gene repression [14], raising the alternative possibility that Ewing Sarcoma metastasis is an active process as in other solid malignancies, but does not rely on (and may even mechanistically oppose) the action of EWS/Fli1. This paradox may in part be reconciled by the fact that the presumptive cells of origin of this cancer (mesenchymal stem cells) possess migratory ability, and express a number of cell adhesion genes implicated in cancer metastasis, including MCAM [50, 80, 81]. Ewing Sarcoma cells may thus have an inherent propensity toward metastasis due to properties inherited from the cell of origin, and partial maintenance of such properties, in the face of EWS/Fli1 opposition, may be sufficient for effective metastasis. Interestingly, a number of the KDM3A-activated pro-metastatic genes identified in our study, including MCAM, are negatively regulated by EWS/Fli1, in part through action of the downstream transcriptional repressor Nkx2.2 [13, 82–84] (Supplemental Figure 5A). Thus, the role of KDM3A in Ewing Sarcoma metastasis, in the context of the EWS/Fli1 fusion, may be in part to maintain sufficient levels of a metastasis-competent gene expression program, including genes such as MCAM, in the face of repression by EWS/Fli1 and/or Nkx2.2 (as summarized in Supplemental Figure 5B).

Metastasis is a highly complex process, involving multiple steps and biological processes in addition to cell migration, a specific phenotype subjected to detailed examination in this study. Notably, efficient metastasis also requires survival of cells in the circulation, independent of surrounding tissue support, and effective outgrowth post organ infiltration. The soft agar assay of anchorage-independent growth can be a surrogate of both metastasis outgrowth and cell survival in the circulation [85]. We have previously observed that KDM3A is a potent promoter of anchorage-independent growth [17], and, notably, MCAM exhibits this property as well (Supplemental Figure 6). Thus, phenotypes in addition to cell migration may contribute to the metastasis-promotional effects of both KDM3A and MCAM, a subject worthy of further examination in future studies.

In summary, the studies herein describe a new metastasis-promoting pathway in Ewing Sarcoma, involving the histone demethylase KDM3A and the cell surface protein MCAM. Given the critical role of metastasis in the aggressive clinical behavior of Ewing Sarcoma, and the recent questions raised about the role of EWS/Ets fusions in this process, understanding of the processes and molecular pathways driving Ewing Sarcoma metastasis assumes substantial importance. Our findings contribute to such understanding and, moreover, since KDM3A and MCAM represent pharmacologically tractable targets, may provide new opportunities for inhibition of metastatic phenotypes in this aggressive cancer.

Materials and Methods

Cell Lines and culture conditions

The Ewing Sarcoma cell lines A673, SK-ES-1 and TC71 have been previously described [17]. TC32 cells were obtained from Dr. Elizabeth Lawlor. Cells were grown in either RPMI (TC32, TC71) or DMEM (all others) with 10% Fetal bovine serum (FBS), 1% Pen/Strep, 10mM Hepes, 1X MEM non-essential amino acids, and 1mM Sodium Pyruvate. All cell

lines were authenticated at our institution by STR profiling and repeatedly verified to be mycoplasma-free.

Global Gene Expression Profiling Analysis

Biological triplicates of A673 cells stably transduced with Scrambled shRNA control, KDM3A sh1 or sh2 were harvested at 70–80% confluence. Total RNA was harvested using TRIzol according to the manufacturer's protocol. The quality and integrity of RNA were verified using the Agilent 2100 Bioanalyzer. For microarray analysis, 250 ng of total RNA was processed using the Whole Transcript Expression kit (Ambion) and Whole Transcript Terminal Labeling kit (Affymetrix). Samples were hybridized to Human Gene 1.1 ST array strips (Affymetrix) and washed, stained, and imaged using the Gene Atlas Personal Microarray System (Affymetrix). Data analysis was performed in Excel and in R (http://www.r-project.org/) using packages publicly available through Bioconductor (http://www.bioconductor.org). As a first step, the microarray imaging data were background corrected and normalized using the gcRMA algorithm [86], resulting in log 2 gene expression values. Functional annotation analysis of differentially expressed genes was performed online with the National Institutes of Health Database for Annotation, Visualization, and Integrated Discovery (DAVID) Web tool (http://david.abcc.ncifcrf.gov/)[87, 88] using Biological Process Gene Ontology (GO)[89] terms. The expression profiling data have been deposited in the NCBI Gene Expression Omnibus database (accession number GSE94619).

Stable silencing of gene expression

shRNA-mediated gene expression silencing via lentiviral delivery was performed as previously described [90]. The control, non-targeting shRNA consisted of a Scrambled sequence (Addgene plasmid 1864;[91]). ShRNAs 1 and 2 for KDM3A correspond to TRCN0000021150 and TRCN0000021152; shRNAs 1 and 2 for MCAM correspond to TRCN0000151337 and TRCN0000275792; shRNAs 1 and 2 for Ets1 correspond to TRCN0000005588 and TRCN0000005591 (all Sigma Mission shRNAs, distributed via the University of Colorado Cancer Center Functional Genomics Core Facility). Following lentiviral transduction, cells were selected with Puromycin (2 μg/ml) for 5 days prior to experiments to gain optimal knock-down of the target genes.

Quantification of RNA expression

Cells were harvested at 70–80% confluence in TRIzol (Invitrogen), and RNA was extracted per manufacturer's instructions. RNA levels of specific transcripts were assessed by qRT-PCR (miScript SYBRgreen, Qiagen) with U6 RNA as the internal control (primers are listed in the Supplemental Methods).

Quantification of protein expression

Protein expression levels were determined by Western blot as previously described [90]. The primary antibodies used were: KDM3A (1:1000, ProMab, #30134), MCAM (1:1000, Proteintech, #17564-1-AP), Ets1 (1:1000, Cell Signaling, #14069), and α-Tubulin (1:20,000, Sigma, #T5168).

Cell migration assays

For Boyden Chamber experiments, cells were washed with serum-free media, and 20,000 cells were plated in replicate in 200 μl of serum-free media in the top of the well insert (8 μm pore, BD Biosciences, #353097). Inserts were then placed in a 24 well companion plate with 600 μl of media containing 5% fetal bovine serum (FBS) as a chemoattractant. After 12 hours, cells were fixed for 20 minutes in 70% ethanol, and unmigrated cells were removed by cleaning the top of the membrane with a cotton swab. Migrated cells were permeabilized for 5 minutes in 0.3% Triton-X in PBS. Cells were stained with 3 μg/ml DAPI in PBS for 20 minutes. Five random fields at 10x power were taken of each well. Quantitation was carried out using the Nikon NLS software object count, and significant differences determined by 1-way ANOVA with multiple comparisons. For IncuCyte experiments, 80,000–100,000 cells were plated in replicate in a 96 well plate and incubated for 6–8 hours. Media was replaced with serum-free media, and the cells were further incubated overnight. The following morning, the confluent monolayer of cells was scratched using the Wound Maker (Essen BioScience), and washed with serum-free media. Cells were then placed in media containing 1% FBS, and incubated in the IncuCyte apparatus with imaging every 4 hours for 24 hours.

Tail vein experimental metastasis assay

Cells were transduced with a lentiviral GFP/luciferase dual reporter (SFG-NES-TGL[92]) and sorted for GFP expression using flow cytometry. GFP-positive cells were then tranduced with either Scrambled control or appropriate targeting shRNA and Puromycin-selected. Cells were harvested, washed, and resuspended in serum-free/antibiotic-free media. 5×10^6 cells per animal were loaded into syringes and injected into the tail vein of NOD/SCID-Gamma mice, times 9–10 animals per group. Sample size was determined based on our past experience. Mice were approximately 3 months in age, male and female; control and experimental groups were matched as equally as possible for sex and precise age. No further randomization was performed. Beginning at 7 days post-injection, mice were imaged every 4–5 days in the IVIS200 bioluminescent imager. Metastasis was quantified in an unblinded analysis by photon flux. Flux values were log transformed to normalize the data, and differences between control and experimental groups were determined using 2-way ANOVA with repeated measures. All animal experiments were in compliance with ethical regulations as approved by our Institutional Animal Care and Use Committee.

Chromatin immunoprecipitation analysis

ChIP analysis of control (Scrambled shRNA), KDM3A knock-down and Ets1 knock-down Ewing Sarcoma A673 cells was performed as described in Supplemental Methods.

Supplementary Material

Refer to Web version on PubMed Central for supplementary material.

Acknowledgments

We wish to thank Elizabeth Wellberg for assistance with gene expression profiling studies; members of the Tobias Neff and Kathrin Bernt laboratories for assistance with chromatin immunoprecipitation studies; Elizabeth Lawlor at the University of Michigan for the TC32 cell line, and tumor expression profiling and patient outcome data[52]; and

Steve Lessnick at Nationwide Children's Hospital for retroviral packaging constructs. We further wish to thank the University of Colorado Cancer Center Flow Cytometry, Functional Genomics, Tissue Culture, DNA Sequencing and Small Animal Imaging Core Facilities, supported by P30-CA046934. Funding support for this work was provided by the Front Range Cancer Challenge, Children's Hospital Colorado Research Institute, University of Colorado School of Medicine Academic Enrichment Funds, and R01-CA183874 (PJ); the Cancer League of Colorado (PJ and MS); and F31-CA203053 (MS).

References

1. Hospital SJCsR. Disease Information, Solid Tumor: Ewing Sarcoma Family Tumors.
2. Gaspar N, Hawkins DS, Dirksen U, Lewis IJ, Ferrari S, Le Deley MC, et al. Ewing Sarcoma: Current Management and Future Approaches Through Collaboration. Journal of clinical oncology : official journal of the American Society of Clinical Oncology. 2015; 33:3036–3046. [PubMed: 26304893]
3. Rodriguez-Galindo C, Navid F, Liu T, Billups CA, Rao BN, Krasin MJ. Prognostic factors for local and distant control in Ewing sarcoma family of tumors. Annals of oncology : official journal of the European Society for Medical Oncology / ESMO. 2008; 19:814–820.
4. Esiashvili N, Goodman M, Marcus RB Jr. Changes in incidence and survival of Ewing sarcoma patients over the past 3 decades: Surveillance Epidemiology and End Results data. Journal of pediatric hematology/oncology. 2008; 30:425–430. [PubMed: 18525458]
5. Grohar PJ, Helman LJ. Prospects and challenges for the development of new therapies for Ewing sarcoma. Pharmacology & therapeutics. 2013; 137:216–224. [PubMed: 23085431]
6. Choy E, Butrynski JE, Harmon DC, Morgan JA, George S, Wagner AJ, et al. Phase II study of olaparib in patients with refractory Ewing sarcoma following failure of standard chemotherapy. BMC cancer. 2014; 14:813. [PubMed: 25374341]
7. Burchill SA. Ewing's sarcoma: diagnostic, prognostic, and therapeutic implications of molecular abnormalities. Journal of clinical pathology. 2003; 56:96–102. [PubMed: 12560386]
8. Riggi N, Knoechel B, Gillespie SM, Rheinbay E, Boulay G, Suva ML, et al. EWS-FLI1 utilizes divergent chromatin remodeling mechanisms to directly activate or repress enhancer elements in Ewing sarcoma. Cancer cell. 2014; 26:668–681. [PubMed: 25453903]
9. Sankar S, Bell R, Stephens B, Zhuo R, Sharma S, Bearss DJ, et al. Mechanism and relevance of EWS/FLI-mediated transcriptional repression in Ewing sarcoma. Oncogene. 2013; 32:5089–5100. [PubMed: 23178492]
10. May WA, Lessnick SL, Braun BS, Klemsz M, Lewis BC, Lunsford LB, et al. The Ewing's sarcoma EWS/FLI-1 fusion gene encodes a more potent transcriptional activator and is a more powerful transforming gene than FLI-1. Molecular and cellular biology. 1993; 13:7393–7398. [PubMed: 8246959]
11. Prieur A, Tirode F, Cohen P, Delattre O. EWS/FLI-1 silencing and gene profiling of Ewing cells reveal downstream oncogenic pathways and a crucial role for repression of insulin-like growth factor binding protein 3. Molecular and cellular biology. 2004; 24:7275–7283. [PubMed: 15282325]
12. Chaturvedi A, Hoffman LM, Welm AL, Lessnick SL, Beckerle MC. The EWS/FLI Oncogene Drives Changes in Cellular Morphology, Adhesion, and Migration in Ewing Sarcoma. Genes & cancer. 2012; 3:102–116. [PubMed: 23050043]
13. Fadul J, Bell R, Hoffman LM, Beckerle MC, Engel ME, Lessnick SL. EWS/FLI utilizes NKX2-2 to repress mesenchymal features of Ewing sarcoma. Genes & cancer. 2015; 6:129–143. [PubMed: 26000096]
14. Pedersen EA, Menon R, Bailey KM, Thomas DG, Van Noord RA, Tran J, et al. Activation of Wnt/beta-Catenin in Ewing Sarcoma Cells Antagonizes EWS/ETS Function and Promotes Phenotypic Transition to More Metastatic Cell States. Cancer research. 2016; 76:5040–5053. [PubMed: 27364557]
15. Feinberg AP, Koldobskiy MA, Gondor A. Epigenetic modulators, modifiers and mediators in cancer aetiology and progression. Nature reviews Genetics. 2016; 17:284–299.

16. Lawlor ER, Thiele CJ. Epigenetic changes in pediatric solid tumors: promising new targets. Clinical cancer research : an official journal of the American Association for Cancer Research. 2012; 18:2768–2779. [PubMed: 22589485]
17. Parrish JK, Sechler M, Winn RA, Jedlicka P. The histone demethylase KDM3A is a microRNA-22-regulated tumor promoter in Ewing Sarcoma. Oncogene. 2015; 34:257–262. [PubMed: 24362521]
18. McFarlane S, Coulter JA, Tibbits P, O'Grady A, McFarlane C, Montgomery N, et al. CD44 increases the efficiency of distant metastasis of breast cancer. Oncotarget. 2015; 6:11465–11476. [PubMed: 25888636]
19. Gao Y, Ruan B, Liu W, Wang J, Yang X, Zhang Z, et al. Knockdown of CD44 inhibits the invasion and metastasis of hepatocellular carcinoma both in vitro and in vivo by reversing epithelial-mesenchymal transition. Oncotarget. 2015; 6:7828–7837. [PubMed: 25797261]
20. Wu GJ, Fu P, Wang SW, Wu MW. Enforced expression of MCAM/MUC18 increases in vitro motility and invasiveness and in vivo metastasis of two mouse melanoma K1735 sublines in a syngeneic mouse model. Molecular cancer research : MCR. 2008; 6:1666–1677. [PubMed: 19010815]
21. Xie S, Luca M, Huang S, Gutman M, Reich R, Johnson JP, et al. Expression of MCAM/MUC18 by human melanoma cells leads to increased tumor growth and metastasis. Cancer research. 1997; 57:2295–2303. [PubMed: 9187135]
22. Tsai HC, Su HL, Huang CY, Fong YC, Hsu CJ, Tang CH. CTGF increases matrix metalloproteinases expression and subsequently promotes tumor metastasis in human osteosarcoma through down-regulating miR-519d. Oncotarget. 2014; 5:3800–3812. [PubMed: 25003330]
23. Rappa G, Green TM, Karbanova J, Corbeil D, Lorico A. Tetraspanin CD9 determines invasiveness and tumorigenicity of human breast cancer cells. Oncotarget. 2015; 6:7970–7991. [PubMed: 25762645]
24. Herr MJ, Kotha J, Hagedorn N, Smith B, Jennings LK. Tetraspanin CD9 promotes the invasive phenotype of human fibrosarcoma cells via upregulation of matrix metalloproteinase-9. PloS one. 2013; 8:e67766. [PubMed: 23840773]
25. Miller NL, Lawson C, Chen XL, Lim ST, Schlaepfer DD. Rgnef (p190RhoGEF) knockout inhibits RhoA activity, focal adhesion establishment, and cell motility downstream of integrins. PloS one. 2012; 7:e37830. [PubMed: 22649559]
26. Yu HG, Nam JO, Miller NL, Tanjoni I, Walsh C, Shi L, et al. p190RhoGEF (Rgnef) promotes colon carcinoma tumor progression via interaction with focal adhesion kinase. Cancer research. 2011; 71:360–370. [PubMed: 21224360]
27. Pavon MA, Arroyo-Solera I, Tellez-Gabriel M, Leon X, Viros D, Lopez M, et al. Enhanced cell migration and apoptosis resistance may underlie the association between high SERPINE1 expression and poor outcome in head and neck carcinoma patients. Oncotarget. 2015; 6:29016–29033. [PubMed: 26359694]
28. Yu XM, Jaskula-Sztul R, Georgen MR, Aburjania Z, Somnay YR, Leverson G, et al. Notch1 Signaling Regulates the Aggressiveness of Differentiated Thyroid Cancer and Inhibits SERPINE1 Expression. Clinical cancer research : an official journal of the American Association for Cancer Research. 2016; 22:3582–3592. [PubMed: 26847059]
29. Sang Y, Chen MY, Luo D, Zhang RH, Wang L, Li M, et al. TEL2 suppresses metastasis by down-regulating SERPINE1 in nasopharyngeal carcinoma. Oncotarget. 2015; 6:29240–29253. [PubMed: 26335051]
30. Du C, Gao Y, Xu S, Jia J, Huang Z, Fan J, et al. KLF5 promotes cell migration by up-regulating FYN in bladder cancer cells. FEBS letters. 2016; 590:408–418. [PubMed: 26786295]
31. Jia L, Zhou Z, Liang H, Wu J, Shi P, Li F, et al. KLF5 promotes breast cancer proliferation, migration and invasion in part by upregulating the transcription of TNFAIP2. Oncogene. 2016; 35:2040–2051. [PubMed: 26189798]
32. Li L, Zhang Z, Ma T, Huo R. PRMT1 regulates tumor growth and metastasis of human melanoma via targeting ALCAM. Molecular medicine reports. 2016; 14:521–528. [PubMed: 27175582]

33. Hansen AG, Arnold SA, Jiang M, Palmer TD, Ketova T, Merkel A, et al. ALCAM/CD166 is a TGF-beta-responsive marker and functional regulator of prostate cancer metastasis to bone. Cancer research. 2014; 74:1404–1415. [PubMed: 24385212]
34. Penna E, Orso F, Cimino D, Vercellino I, Grassi E, Quaglino E, et al. miR-214 coordinates melanoma progression by upregulating ALCAM through TFAP2 and miR-148b downmodulation. Cancer research. 2013; 73:4098–4111. [PubMed: 23667173]
35. Shi, W., Zhang, C., Chen, Z., Chen, H., Liu, L., Meng, Z. Oncotarget. 2016. Cyr61-positive cancer stem-like cells enhances distal metastases of pancreatic cancer.
36. Hou CH, Lin FL, Hou SM, Liu JF. Cyr61 promotes epithelial-mesenchymal transition and tumor metastasis of osteosarcoma by Raf-1/MEK/ERK/Elk-1/TWIST-1 signaling pathway. Molecular cancer. 2014; 13:236. [PubMed: 25326651]
37. Habel N, Vilalta M, Bawa O, Opolon P, Blanco J, Fromigue O. Cyr61 silencing reduces vascularization and dissemination of osteosarcoma tumors. Oncogene. 2015; 34:3207–3213. [PubMed: 25065593]
38. Oskarsson T, Acharyya S, Zhang XH, Vanharanta S, Tavazoie SF, Morris PG, et al. Breast cancer cells produce tenascin C as a metastatic niche component to colonize the lungs. Nature medicine. 2011; 17:867–874.
39. Paron I, Berchtold S, Voros J, Shamarla M, Erkan M, Hofler H, et al. Tenascin-C enhances pancreatic cancer cell growth and motility and affects cell adhesion through activation of the integrin pathway. PloS one. 2011; 6:e21684. [PubMed: 21747918]
40. Dittmer J. The role of the transcription factor Ets1 in carcinoma. Seminars in cancer biology. 2015; 35:20–38. [PubMed: 26392377]
41. Zheng L, Qi T, Yang D, Qi M, Li D, Xiang X, et al. microRNA-9 suppresses the proliferation, invasion and metastasis of gastric cancer cells through targeting cyclin D1 and Ets1. PloS one. 2013; 8:e55719. [PubMed: 23383271]
42. Lim SY, Yuzhalin AE, Gordon-Weeks AN, Muschel RJ. Targeting the CCL2-CCR2 signaling axis in cancer metastasis. Oncotarget. 2016; 7:28697–28710. [PubMed: 26885690]
43. Yang J, Lv X, Chen J, Xie C, Xia W, Jiang C, et al. CCL2-CCR2 axis promotes metastasis of nasopharyngeal carcinoma by activating ERK1/2-MMP2/9 pathway. Oncotarget. 2016; 7:15632–15647. [PubMed: 26701209]
44. Kitamura T, Qian BZ, Soong D, Cassetta L, Noy R, Sugano G, et al. CCL2-induced chemokine cascade promotes breast cancer metastasis by enhancing retention of metastasis-associated macrophages. The Journal of experimental medicine. 2015; 212:1043–1059. [PubMed: 26056232]
45. Park JS, Lee JH, Lee YS, Kim JK, Dong SM, Yoon DS. Emerging role of LOXL2 in the promotion of pancreas cancer metastasis. Oncotarget. 2016; 7:42539–42552. [PubMed: 27285767]
46. Peng DH, Ungewiss C, Tong P, Byers LA, Wang J, Canales JR, et al. ZEB1 induces LOXL2-mediated collagen stabilization and deposition in the extracellular matrix to drive lung cancer invasion and metastasis. Oncogene. 2016
47. Moreno-Bueno G, Salvador F, Martin A, Floristan A, Cuevas EP, Santos V, et al. Lysyl oxidase-like 2 (LOXL2), a new regulator of cell polarity required for metastatic dissemination of basal-like breast carcinomas. EMBO molecular medicine. 2011; 3:528–544. [PubMed: 21732535]
48. Liang XH, Zhang GX, Zeng YB, Yang HF, Li WH, Liu QL, et al. LIM protein JUB promotes epithelial-mesenchymal transition in colorectal cancer. Cancer science. 2014; 105:660–666. [PubMed: 24673742]
49. Hou Z, Peng H, Ayyanathan K, Yan KP, Langer EM, Longmore GD, et al. The LIM protein AJUBA recruits protein arginine methyltransferase 5 to mediate SNAIL-dependent transcriptional repression. Molecular and cellular biology. 2008; 28:3198–3207. [PubMed: 18347060]
50. Wang Z, Yan X. CD146, a multi-functional molecule beyond adhesion. Cancer letters. 2013; 330:150–162. [PubMed: 23266426]
51. Orentas RJ, Yang JJ, Wen X, Wei JS, Mackall CL, Khan J. Identification of cell surface proteins as potential immunotherapy targets in 12 pediatric cancers. Frontiers in oncology. 2012; 2:194. [PubMed: 23251904]
52. Volchenboum SL, Andrade J, Huang L, Barkauskas DA, Krailo M, Womer RB, et al. Gene Expression Profiling of Ewing Sarcoma Tumors Reveals the Prognostic Importance of Tumor-

Stromal Interactions: A Report from the Children's Oncology Group. The journal of pathology Clinical research. 2015; 1:83–94. [PubMed: 26052443]

53. Douglas D, Hsu JH, Hung L, Cooper A, Abdueva D, van Doorninck J, et al. BMI-1 promotes ewing sarcoma tumorigenicity independent of CDKN2A repression. Cancer research. 2008; 68:6507–6515. [PubMed: 18701473]
54. Richter GH, Plehm S, Fasan A, Rossler S, Unland R, Bennani-Baiti IM, et al. EZH2 is a mediator of EWS/FLI1 driven tumor growth and metastasis blocking endothelial and neuro-ectodermal differentiation. Proceedings of the National Academy of Sciences of the United States of America. 2009; 106:5324–5329. [PubMed: 19289832]
55. Bennani-Baiti IM, Machado I, Llombart-Bosch A, Kovar H. Lysine-specific demethylase 1 (LSD1/KDM1A/AOF2/BHC110) is expressed and is an epigenetic drug target in chondrosarcoma, Ewing's sarcoma, osteosarcoma, and rhabdomyosarcoma. Human pathology. 2012; 43:1300–1307. [PubMed: 22245111]
56. Patel M, Simon JM, Iglesia MD, Wu SB, McFadden AW, Lieb JD, et al. Tumor-specific retargeting of an oncogenic transcription factor chimera results in dysregulation of chromatin and transcription. Genome research. 2012; 22:259–270. [PubMed: 22086061]
57. Svoboda LK, Harris A, Bailey NJ, Schwentner R, Tomazou E, von Levetzow C, et al. Overexpression of HOX genes is prevalent in Ewing sarcoma and is associated with altered epigenetic regulation of developmental transcription programs. Epigenetics : official journal of the DNA Methylation Society. 2014; 9:1613–1625.
58. Ramadoss S, Sen S, Ramachandran I, Roy S, Chaudhuri G, Farias-Eisner R. Lysine-specific demethylase KDM3A regulates ovarian cancer stemness and chemoresistance. Oncogene. 2016
59. Ramadoss S, Guo G, Wang CY. Lysine demethylase KDM3A regulates breast cancer cell invasion and apoptosis by targeting histone and the non-histone protein p53. Oncogene. 2016
60. Mahajan K, Lawrence HR, Lawrence NJ, Mahajan NP. ACK1 tyrosine kinase interacts with histone demethylase KDM3A to regulate the mammary tumor oncogene HOXA1. The Journal of biological chemistry. 2014; 289:28179–28191. [PubMed: 25148682]
61. Cho HS, Toyokawa G, Daigo Y, Hayami S, Masuda K, Ikawa N, et al. The JmjC domain-containing histone demethylase KDM3A is a positive regulator of the G1/S transition in cancer cells via transcriptional regulation of the HOXA1 gene. International journal of cancer Journal international du cancer. 2012; 131:E179–189. [PubMed: 22020899]
62. Tee AE, Ling D, Nelson C, Atmadibrata B, Dinger ME, Xu N, et al. The histone demethylase JMJD1A induces cell migration and invasion by up-regulating the expression of the long noncoding RNA MALAT1. Oncotarget. 2014; 5:1793–1804. [PubMed: 24742640]
63. Ohguchi H, Hideshima T, Bhasin MK, Gorgun GT, Santo L, Cea M, et al. The KDM3A-KLF2-IRF4 axis maintains myeloma cell survival. Nature communications. 2016; 7:10258.
64. Shih IM, Elder DE, Speicher D, Johnson JP, Herlyn M. Isolation and functional characterization of the A32 melanoma-associated antigen. Cancer research. 1994; 54:2514–2520. [PubMed: 8162602]
65. Lin Y, Wu X, Shen Y, Bu P, Yang D, Yan X. A novel antibody AA98 V(H)/L directed against CD146 efficiently inhibits angiogenesis. Anticancer research. 2007; 27:4219–4224. [PubMed: 18225593]
66. Jouve N, Despoix N, Espeli M, Gauthier L, Cypowyj S, Fallague K, et al. The involvement of CD146 and its novel ligand Galectin-1 in apoptotic regulation of endothelial cells. The Journal of biological chemistry. 2013; 288:2571–2579. [PubMed: 23223580]
67. Bardin N, Blot-Chabaud M, Despoix N, Kebir A, Harhouri K, Arsanto JP, et al. CD146 and its soluble form regulate monocyte transendothelial migration. Arteriosclerosis, thrombosis, and vascular biology. 2009; 29:746–753.
68. Zhang X, Wang Z, Kang Y, Li X, Ma X, Ma L. MCAM expression is associated with poor prognosis in non-small cell lung cancer. Clinical & translational oncology : official publication of the Federation of Spanish Oncology Societies and of the National Cancer Institute of Mexico. 2014; 16:178–183.
69. Zeng Q, Li W, Lu D, Wu Z, Duan H, Luo Y, et al. CD146, an epithelial-mesenchymal transition inducer, is associated with triple-negative breast cancer. Proceedings of the National Academy of Sciences of the United States of America. 2012; 109:1127–1132. [PubMed: 22210108]

70. Imbert AM, Garulli C, Choquet E, Koubi M, Aurrand-Lions M, Chabannon C. CD146 expression in human breast cancer cell lines induces phenotypic and functional changes observed in Epithelial to Mesenchymal Transition. PloS one. 2012; 7:e43752. [PubMed: 22952755]
71. Jouve N, Bachelier R, Despoix N, Blin MG, Matinzadeh MK, Poitevin S, et al. CD146 mediates VEGF-induced melanoma cell extravasation through FAK activation. International journal of cancer Journal international du cancer. 2015; 137:50–60. [PubMed: 25449773]
72. Liu XS, Genet MD, Haines JE, Mehanna EK, Wu S, Chen HI, et al. ZBTB7A Suppresses Melanoma Metastasis by Transcriptionally Repressing MCAM. Molecular cancer research : MCR. 2015; 13:1206–1217. [PubMed: 25995384]
73. Schiano C, Grimaldi V, Casamassimi A, Infante T, Esposito A, Giovane A, et al. Different expression of CD146 in human normal and osteosarcoma cell lines. Med Oncol. 2012; 29:2998–3002. [PubMed: 22271434]
74. Dittmer J. The biology of the Ets1 proto-oncogene. Molecular cancer. 2003; 2:29. [PubMed: 12971829]
75. Heidenreich B, Rachakonda PS, Hemminki K, Kumar R. TERT promoter mutations in cancer development. Current opinion in genetics & development. 2014; 24:30–37. [PubMed: 24657534]
76. Zhan M, Wen F, Liu L, Chen Z, Wei H, Zhou H. JMJD1A promotes tumorigenesis and forms a feedback loop with EZH2/let-7c in NSCLC cells. Tumour biology : the journal of the International Society for Oncodevelopmental Biology and Medicine. 2016
77. Yang H, Liu Z, Yuan C, Zhao Y, Wang L, Hu J, et al. Elevated JMJD1A is a novel predictor for prognosis and a potential therapeutic target for gastric cancer. International journal of clinical and experimental pathology. 2015; 8:11092–11099. [PubMed: 26617828]
78. Wade MA, Jones D, Wilson L, Stockley J, Coffey K, Robson CN, et al. The histone demethylase enzyme KDM3A is a key estrogen receptor regulator in breast cancer. Nucleic acids research. 2015; 43:196–207. [PubMed: 25488809]
79. Pa M, Naizaer G, Seyiti A, Kuerbang G. KDM3A confers metastasis and chemoresistance in epithelial ovarian cancer. Journal of molecular histology. 2015
80. Sohni A, Verfaillie CM. Mesenchymal stem cells migration homing and tracking. Stem cells international. 2013; 2013:130763. [PubMed: 24194766]
81. Steingen C, Brenig F, Baumgartner L, Schmidt J, Schmidt A, Bloch W. Characterization of key mechanisms in transmigration and invasion of mesenchymal stem cells. Journal of molecular and cellular cardiology. 2008; 44:1072–1084. [PubMed: 18462748]
82. Smith R, Owen LA, Trem DJ, Wong JS, Whangbo JS, Golub TR, et al. Expression profiling of EWS/FLI identifies NKX2. 2 as a critical target gene in Ewing's sarcoma. Cancer cell. 2006; 9:405–416. [PubMed: 16697960]
83. Chaturvedi A, Hoffman LM, Jensen CC, Lin YC, Grossmann AH, Randall RL, et al. Molecular dissection of the mechanism by which EWS/FLI expression compromises actin cytoskeletal integrity and cell adhesion in Ewing sarcoma. Molecular biology of the cell. 2014; 25:2695–2709. [PubMed: 25057021]
84. Owen LA, Kowalewski AA, Lessnick SL. EWS/FLI mediates transcriptional repression via NKX2. 2 during oncogenic transformation in Ewing's sarcoma. PloS one. 2008; 3:e1965. [PubMed: 18414662]
85. Li X, Xu Z, Du W, Zhang Z, Wei Y, Wang H, et al. Aiolos promotes anchorage independence by silencing p66Shc transcription in cancer cells. Cancer cell. 2014; 25:575–589. [PubMed: 24823637]
86. Wu ZJ, Irizarry RA, Gentleman R, Martinez-Murillo F, Spencer F. A model-based background adjustment for oligonucleotide expression arrays. J Am Stat Assoc. 2004; 99:909–917.
87. Dennis G Jr, Sherman BT, Hosack DA, Yang J, Gao W, Lane HC, et al. DAVID: Database for Annotation, Visualization, and Integrated Discovery. Genome biology. 2003; 4:P3. [PubMed: 12734009]
88. Huang da W, Sherman BT, Lempicki RA. Systematic and integrative analysis of large gene lists using DAVID bioinformatics resources. Nat Protoc. 2009; 4:44–57. [PubMed: 19131956]

89. Ashburner M, Ball CA, Blake JA, Botstein D, Butler H, Cherry JM, et al. Gene ontology: tool for the unification of biology. The Gene Ontology Consortium Nature genetics. 2000; 25:25–29. [PubMed: 10802651]

90. McKinsey EL, Parrish JK, Irwin AE, Niemeyer BF, Kern HB, Birks DK, et al. A novel oncogenic mechanism in Ewing sarcoma involving IGF pathway targeting by EWS/Fli1-regulated microRNAs. Oncogene. 2011; 30:4910–4920. [PubMed: 21643012]

91. Sarbassov DD, Guertin DA, Ali SM, Sabatini DM. Phosphorylation and regulation of Akt/PKB by the rictor-mTOR complex. Science. 2005; 307:1098–1101. [PubMed: 15718470]

92. Ponomarev V, Doubrovin M, Serganova I, Vider J, Shavrin A, Beresten T, et al. A novel triple-modality reporter gene for whole-body fluorescent, bioluminescent, and nuclear noninvasive imaging. European journal of nuclear medicine and molecular imaging. 2004; 31:740–751. [PubMed: 15014901]

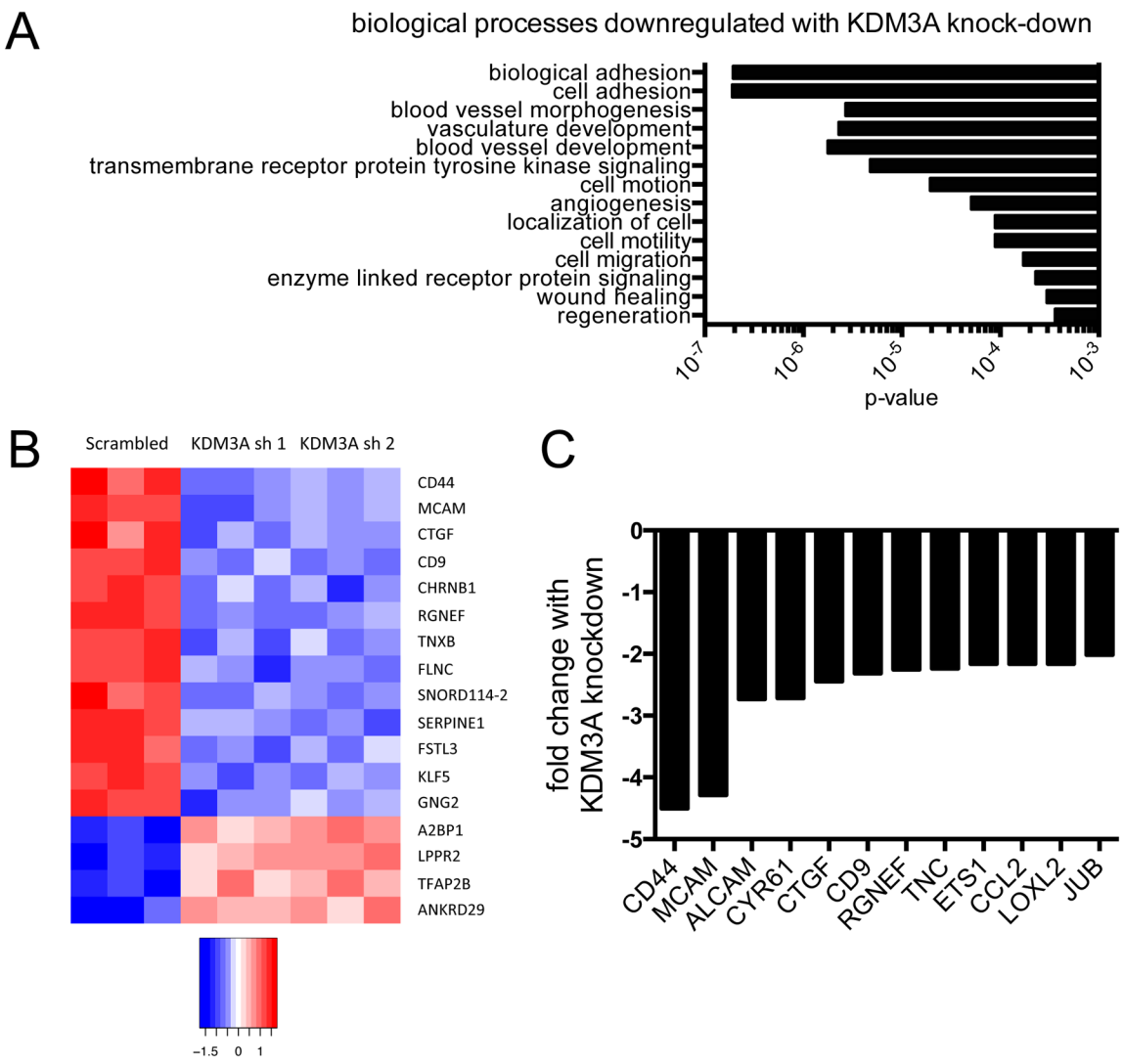

Figure 1.

Changes in gene expression upon stable depletion of KDM3A in A673 cells. A) GO terms (biological processes) significantly enriched among downregulated genes in KDM3A knock-down cells relative to control (Scrambled shRNA) cells, as determined by DAVID functional annotation analysis. B) Heatmap of top differentially expressed genes (FDR < 0.1) in KDM3A knock-down cells relative to control (Scrambled shRNA) cells. C) Individual genes contributing to GO term enrichment in “A”, that have been implicated in metastasis promotion in other cancers and were downregulated 2-fold or more upon KDM3A knock-down.

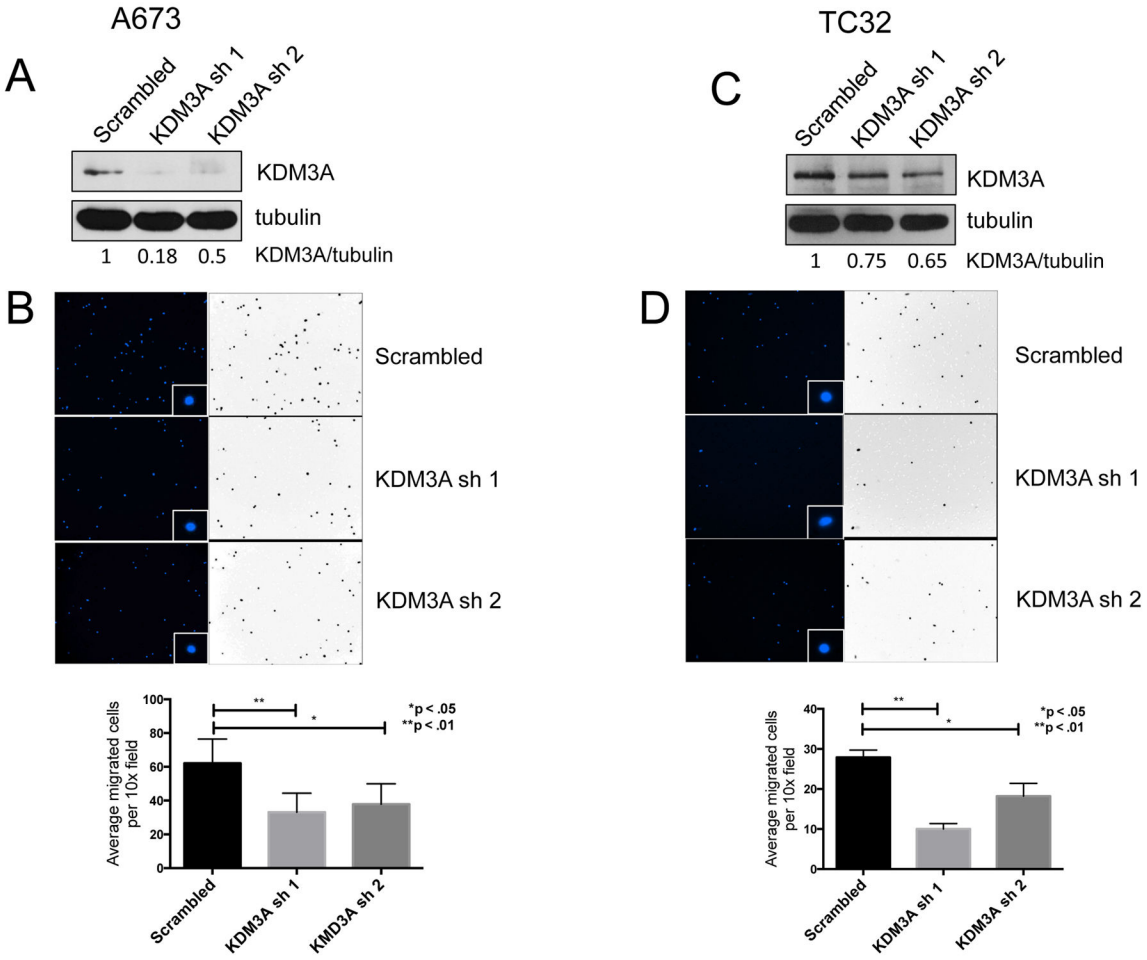

Figure 2.

Stable depletion of KDM3A inhibits cell migration. A and C) KDM3A knock-down in A673 and TC32 cells, as determined by immunoblotting and quantified by densitometry. B and D) Cell migration in a Boyden chamber assay at 12 hours in control (Scrambled shRNA) and KDM3A knock-down A673 and TC32 cells. Representative images of DAPI-stained nuclei of migrated cells (left panels, including high-magnification images of nuclear staining in inset), pseudo-colored black on a white background for ease of visualization(right panels), from one experiment are shown; quantifications represent mean and standard error of the mean from three or more experiments, each performed in duplicate; statistical significance was determined using a 1-way ANOVA with multiple comparisons.

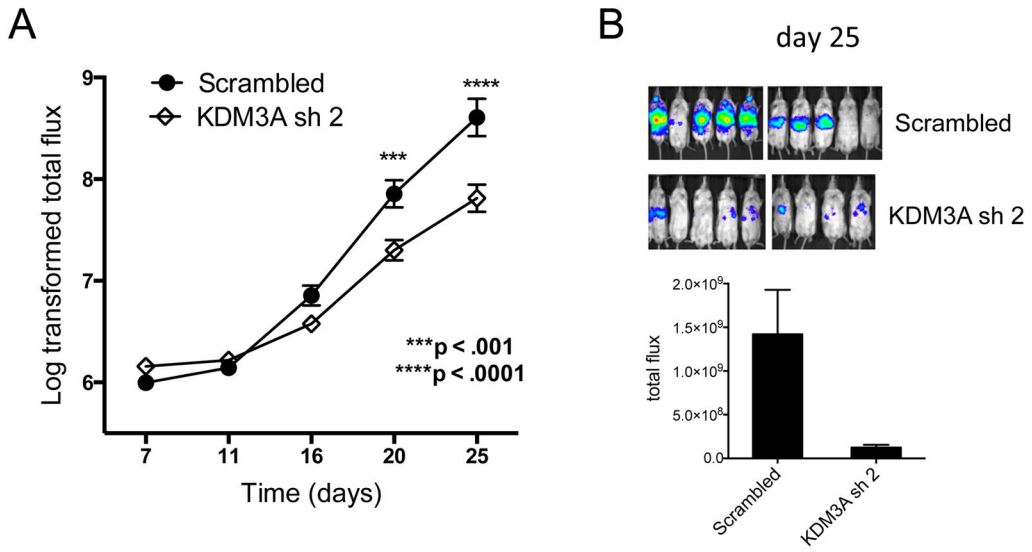

Figure 3.

Stable depletion of KDM3A decreases experimental, post-intravasation, metastasis *in vivo*. 5 × 10^6 luciferase-tagged control (Scrambled shRNA) and KDM3A knock-down A673 cells were injected into the tail veins of NOD/SCID-Gamma mice, and metastatic tumor burden was assessed quantitatively using IVIS imaging. Metastasis was quantified by photon flux and differences between control and experimental groups were determined. A) Data from full experimental time course plotted as mean and standard error of log transformed photon flux; statistical significance was determined using 2-way ANOVA with repeated measures. B) Representative photon flux imaging data, and corresponding quantification (on linear scale), from day 25 of experiment.

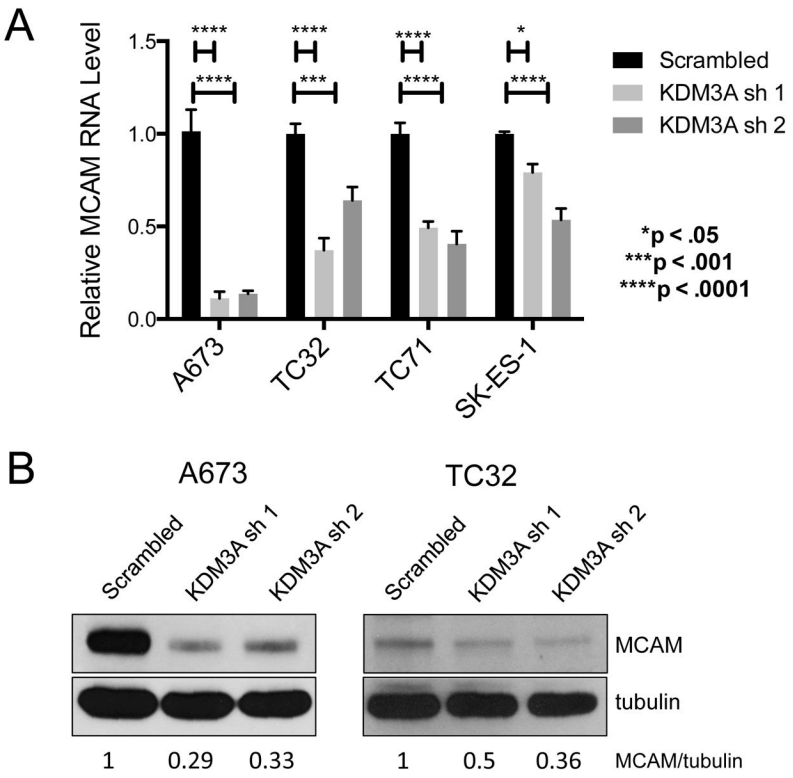

Figure 4.

KDM3A regulates MCAM expression. A) MCAM mRNA levels in control (Scrambled shRNA) and KDM3A knock-down cells, as measured in four different Ewing Sarcoma cell lines by qRT-PCR. B) MCAM protein levels in control (Scrambled shRNA) and KDM3A knock-down cells in A673 and TC32 cells.

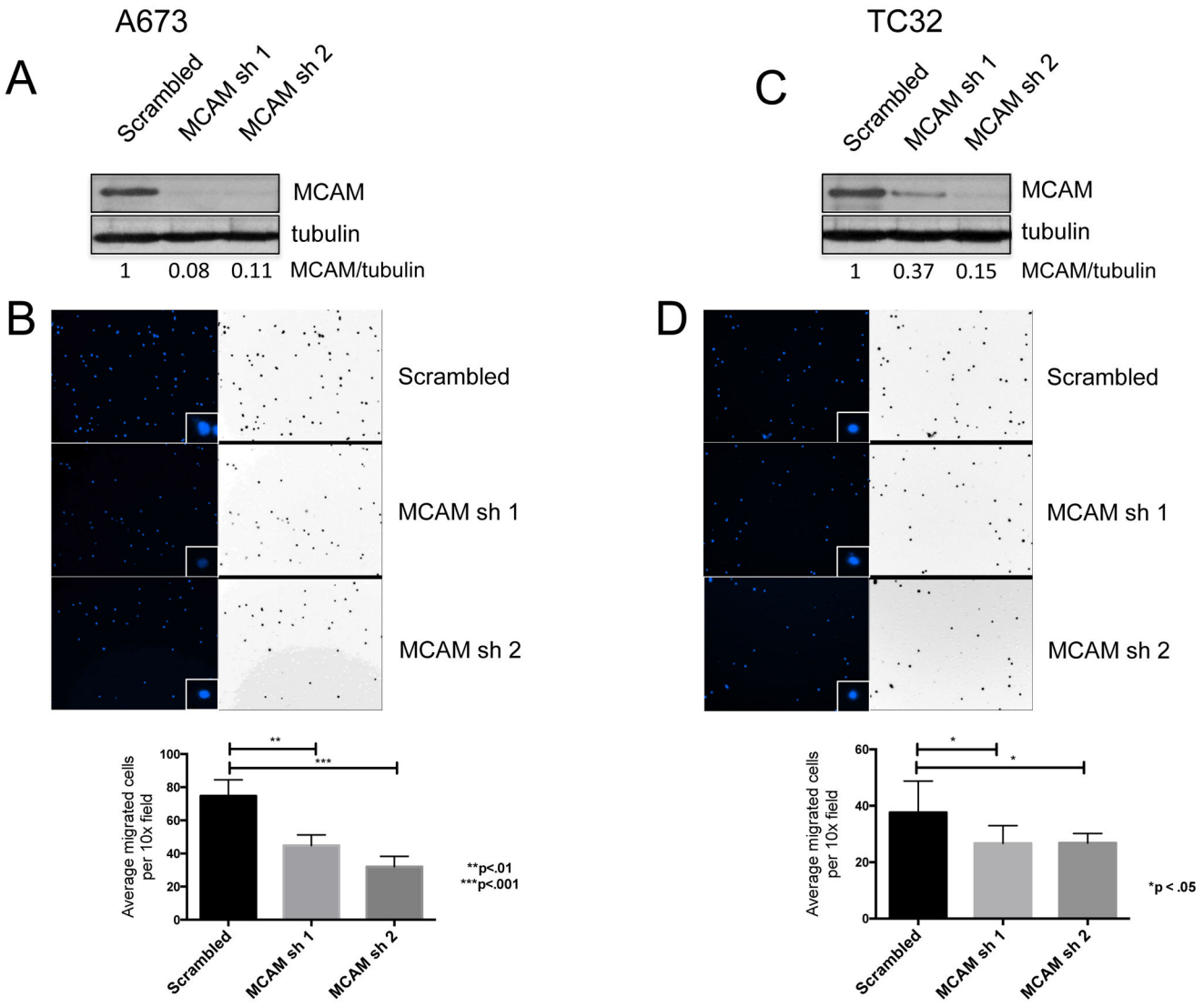

Figure 5.

Stable depletion of MCAM inhibits cell migration. A and C) MCAM knock-down in A673 and TC32 cells, as determined by immunoblotting and quantified by densitometry. B and D) Cell migration in a Boyden chamber assay at 12 hours in control (Scrambled shRNA) and MCAM knock-down A673 and TC32 cells. Representative images of DAPI-stained nuclei of migrated cells (left panels, including high-magnification images of nuclear staining in inset), pseudo-colored black on a white background for ease of visualization (right panels), from one experiment are shown; quantifications represent mean and standard error of the mean from three or more experiments, each performed in duplicate; statistical significance was determined using a 1-way ANOVA with multiple comparisons.

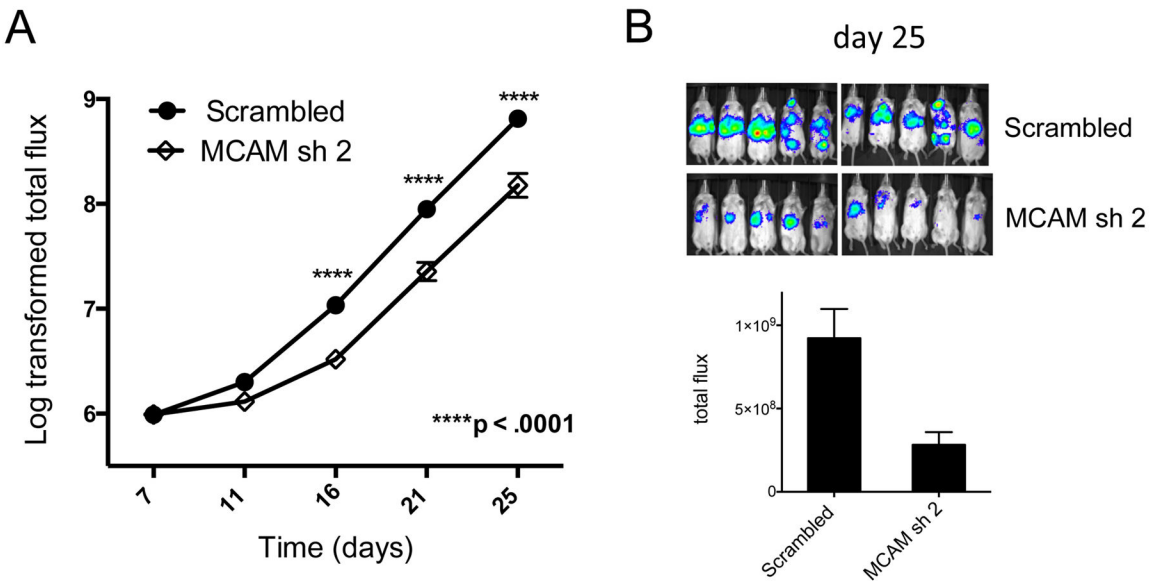

Figure 6.

Stable depletion of MCAM decreases metastasis *in vivo*. 5×10^6 luciferase-tagged control (Scrambled shRNA) and MCAM knock-down A673 cells were injected into the tail veins of NOD/SCID-Gamma mice, and metastatic tumor burden was assessed quantitatively using IVIS imaging. Metastasis was quantified by photon flux and differences between control and experimental groups were determined. A) Data from full experimental time course plotted as mean and standard error of log transformed photon flux; statistical significance was determined using 2-way ANOVA with repeated measures. B) Representative photon flux imaging data, and corresponding quantification (on linear scale), from day 25 of experiment.

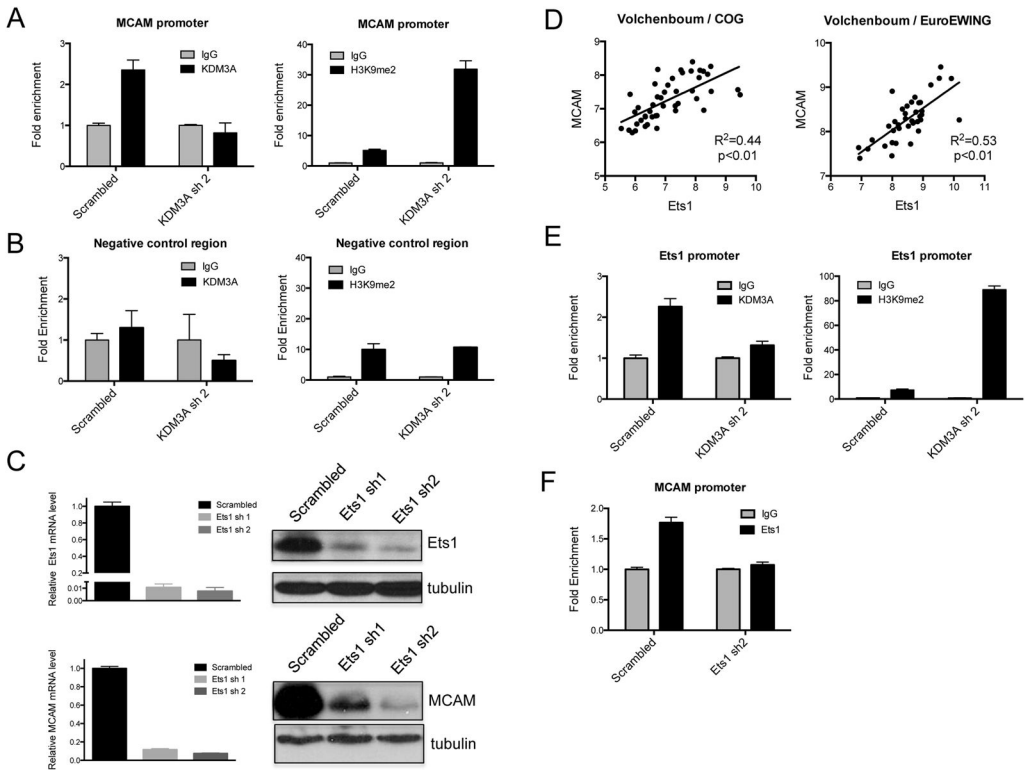

Figure 7.

KDM3A binds and demethylates MCAM and Ets1 promoters, and Ets1 binds the MCAM promoter and regulates MCAM expression. A and E) Chromatin Immunoprecipitation (ChIP) followed by qPCR with KDM3A (left panel) and H3K9me2 (right panel) antibodies, and appropriate negative control antibodies (species-matched IgG), in control (Scrambled shRNA) and KDM3A knock-down A673 cells. Data are plotted as fold-enrichment of specific antibody binding over IgG control, shown as mean and standard deviation of replicate qPCR reactions from 2 independent ChIP experiments; data for MCAM promoter (A) and Ets1 promoter (E). B) ChIP-qPCR data for KDM3A and H3K9me2 at a negative control region (10 Kbp upstream of MCAM transcription start site). C) Ets1 (top panels) and MCAM (bottom panels) RNA and protein levels in control (Scrambled shRNA) and Ets1 knock-down A673 cells, as determined by qRT-PCR and immunoblotting respectively. D) Correlation of MCAM and Ets1 RNA levels in Ewing Sarcoma primary patient tumors (data from Volchenboum et al, J. Pathol. 2015). F) ChIP-qPCR for Ets1 at the MCAM promoter, in Scrambled control and Ets1 knock-down cells, performed and analyzed as in A and E.

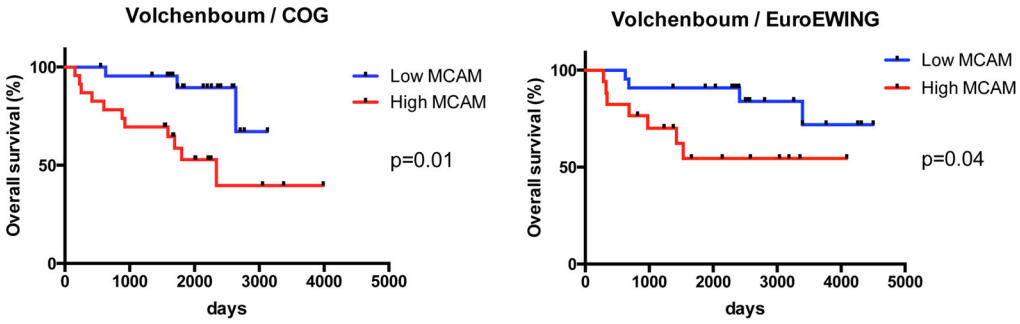

Figure 8.

High MCAM expression in Ewing Sarcoma primary patient tumors is associated with poor survival. Kaplan-Meier analysis of overall Ewing Sarcoma patient survival based on stratification by high (above mean) and low (below mean) MCAM RNA levels in primary tumors (data from Volchenboum et al, J. Pathol. 2015). Significance was determined by a Log-rank (Mantel-Cox) test.